Article

Superphenylphosphines: Nanographene-based Ligands That Control Coordination Geometry and Drive Supramolecular Assembly

Jordan Neale Smith, James M. Hook, and Nigel T. Lucas

J. Am. Chem. Soc., **Just Accepted Manuscript** • DOI: 10.1021/jacs.7b12251 • Publication Date (Web): 18 Dec 2017

Superphenylphosphines: Nanographene-based Ligands That Control Coordination Geometry and Drive Supramolecular Assembly

Jordan N. Smith,[†] James M. Hook[‡] and Nigel T. Lucas[*,†]

[†]MacDiarmid Institute for Advanced Materials and Nanotechnology, Department of Chemistry, University of Otago, Union Place, Dunedin 9016, New Zealand

[‡]Mark Wainwright Analytical Centre, University of New South Wales, Sydney, NSW 2052, Australia.

ABSTRACT: Tertiary phosphines remain widely utilized in synthesis, most notably as supporting ligands in metal complexes. A series of triarylphosphines bearing one to three hexa-*peri*-hexabenzocoronene (HBC) substituents has been prepared by an efficient divergent route. These "superphenylphosphines", $P\{HBC(t\text{-}Bu)_5\}_nPh_{3-n}$ (n = 1-3), form the palladium complexes $Pd_2Cl_2L_2$ and $Pd_2Cl_4L_2$ where the isomer distribution in solution is dependent on the number of HBC substituents. The crystalline structures of five complexes all show intramolecular π-stacking between HBC-phosphines to form a supramolecular bidentate-like ligand that distorts the metal coordination geometry. When n = 2 or 3, the additional HBC substituents engage in intermolecular π-stacking to assemble the complexes into continuous ribbons or sheets. The phosphines adopt HBC's characteristics including strong optical absorption, green emission, and redox activity.

INTRODUCTION

An important class of organophosphorus compounds across all areas of chemical synthesis, phosphines remain ubiquitous as ligands in coordination and organometallic chemistry.[1-3] The status of tertiary phosphines as excellent supporting ligands in homogeneous catalysis is attributed to the broad tunability of their electronic and steric characteristics through modification of the three organic substituents.[4] Beyond applications in transition metal catalysis, phosphines and related structures have received attention as soft donor ligands in multimetallic supramolecular coordination assemblies,[5] as stabilizing ligands for metal clusters and nanoparticles,[6] as bases in frustrated Lewis pairs[7] and as active materials in a range of optoelectronic applications.[8-9]

Chelating bidentate ligands typically produce a more rigid coordination environment at metal centers, with the 'bite angle' of the donor atoms programmed by the ligand's covalent backbone.[4, 10] An alternative to conventional chelating ligands is the self-assembly of monodentate ligands through non-covalent interactions.[11-14] Aromatic groups and interactions involving π-systems can critically affect reactivity within the metal coordination sphere,[15] however, π-π interactions are rarely utilized for directed assembly of supramolecular chelate ligands, attributed to the relative weakness of the interactions for small neutral aromatic substituents.[16] Although polarized C–H bonds provide directionality through favourable offset face-to-face (π-stacking) and edge-to-face motifs,[16] multiple interactions need to act in concert to direct supramolecular order.[17] For large polycyclic aromatic hydrocarbons (PAHs), the dominant face-to-face arrangement results in persistent columnar structures in crystalline[18-19] and liquid crystalline[20-21] phases. Soluble PAHs with long alkyl chains facilitate solution processing of these carbon-rich materials into highly-ordered semiconducting films, driven by π-stacking aggregation.[22-23]

Herein we report a series of triarylphosphines (**1-3**) that bear large PAH substituents capable of engaging in robust π-stacked interactions (Chart 1). We have chosen hexa-*peri*-hexabenzocoronene (HBC) as the extended aromatic fragment to attach directly to the phosphorus donor atom. HBCs have attracted attention because of their electronic and optical properties, their high thermal and chemical stability, as nano-sized graphene models and for their propensity to reliably self-assemble through π-stacking.[23-26] As a Clar benzenoid PAH[27] with seven aromatic sextets, HBC can be regarded as a homologue of benzene, which, along with its hexagonal symmetry and readily functionalised peripheral sites, has earned it the name "superbenzene";[26,28-30] accordingly, our HBC-phosphines have been dubbed "superphenylphosphines".

Chart 1. Structures of superphenylphosphines 1-3 and related compounds.

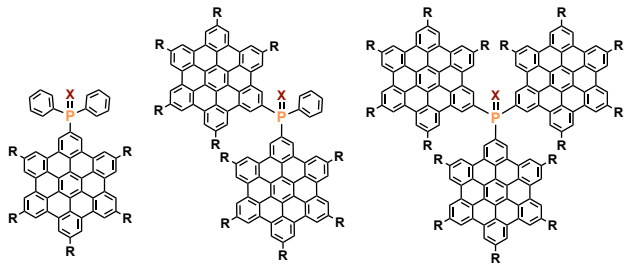

R = *t*-Bu, **X** = –; **a**, **X** = O; **b**, **X** = BH_3; **c**, **X** = Se

A number of metal complexes with ligands bearing an HBC substituent have been reported,[25, 31-38] along with *N*-heteroaromatic analogues;[39-41] in examples where a crystal structure was obtained, the HBC groups play a leading role in directing the supramolecular structure. Challenges exist in synthesising HBC ligands, especially those with multiple HBC substituents, as insolubility can result from the extended π-stacking, thus limiting further application. Our choice of alkyl substituent and synthetic approach has allowed us to manage the issue of solubility, while harnessing the robust interactions between HBCs to influence both coordination geometry and bulk order of the superphenylphosphine complexes.

RESULTS AND DISCUSSION

Phosphine Synthesis. Mono-HBC-functionalized superphenylphosphine **1** was synthesized first, with an emphasis on finding methods that could be translated to higher structures **2** and **3**. Rather than introduce the HBC fragment directly onto phosphorus, synthesis of the hexaphenylbenzene (HPB)-phosphine oxide **4a** prior to oxidative cyclodehydrogenation ensures adequate solubility through this core coupling step (Scheme 1). Of several approaches investigated, the highest yields of **4a** were achieved using a divergent route starting from phosphine oxide **10** in a Sonogashira coupling, followed by Diels-Alder cycloaddition reaction with **12**. Cyclodehydrogenation of HPB **4a** to HBC **1a** was achieved in 96% yield using $FeCl_3$/nitromethane, followed by extractive workup and chromatography; pleasingly, the P=O moiety did not interfere with this key step. The solubility of **1a** in common organic solvents is good (toluene, THF, CH_2Cl_2, $CHCl_3$) to excellent (CS_2, 1,2-dichlorobenzene).

Extension of the methods developed for phosphine oxide **1a** to the synthesis of **2a** and **3a** was relatively straightforward (Scheme 1). Cycloaddition of the acetylenes **13** and **14** with **8** returned gram-scale quantities of **5a** and **6a**. Following oxidative cyclodehydrogenation, **2a** and **3a** were formed in excellent yields, especially noteworthy considering these steps involve the formation of 12 and 18 new bonds, respectively. While **2a** demonstrated similar solubility to **1a**, **3a** was less soluble in chloroalkane solvents (CH_2Cl_2, $CHCl_3$) and could not be easily extracted without the addition of CS_2. The preferred method for isolation of **3a** was precipitation from the reaction mixture with methanol.

All new compounds were fully characterized by ^1H, ^{13}C and ^{31}P NMR, and signals assigned with the use of 2-D experiments as described in the Supporting Information. The ^{31}P NMR resonance frequencies of the phosphine oxides **1a**–**3a** show an increase across the series (δ_{1a} = 32.8; δ_{2a} = 35.9; δ_{3a} = 38.6 ppm), indicating significant changes in the magnetic environment at phosphorus, and consistent with the additive anisotropic de-shielding contributions from the HBC cores. The ^1H NMR spectra show aromatic resonances attributed to core HBC protons, along with distinct phenyl signals for **1a** and **2a** (Figure 1). Furthermore, the HBC protons *ortho* to phosphorus appear as doublets (J_{HP} = 13.5 Hz) that collapse with ^{31}P decoupling, and show a downfield shift across the series (Figure 1). In contrast, the *t*-Bu groups adjacent to phosphorus show an additive upfield shift corresponding to the shielding effect of the adjacent π-electron-rich HBC surfaces. Although the solid state structure of **3a** (vide infra) shows a chiral propeller motif, NMR reveals that the HBC(*t*-Bu)$_5$ fragments have sufficient rotational freedom to racemize in solution with magnetic equivalence about the 2-fold P-HBC axis. MALDI-TOF mass spectra show a single peak envelope corresponding to the molecular ion in each case (see Supporting Information).

Scheme 1. Synthesis of phosphine oxides 1a–3a.

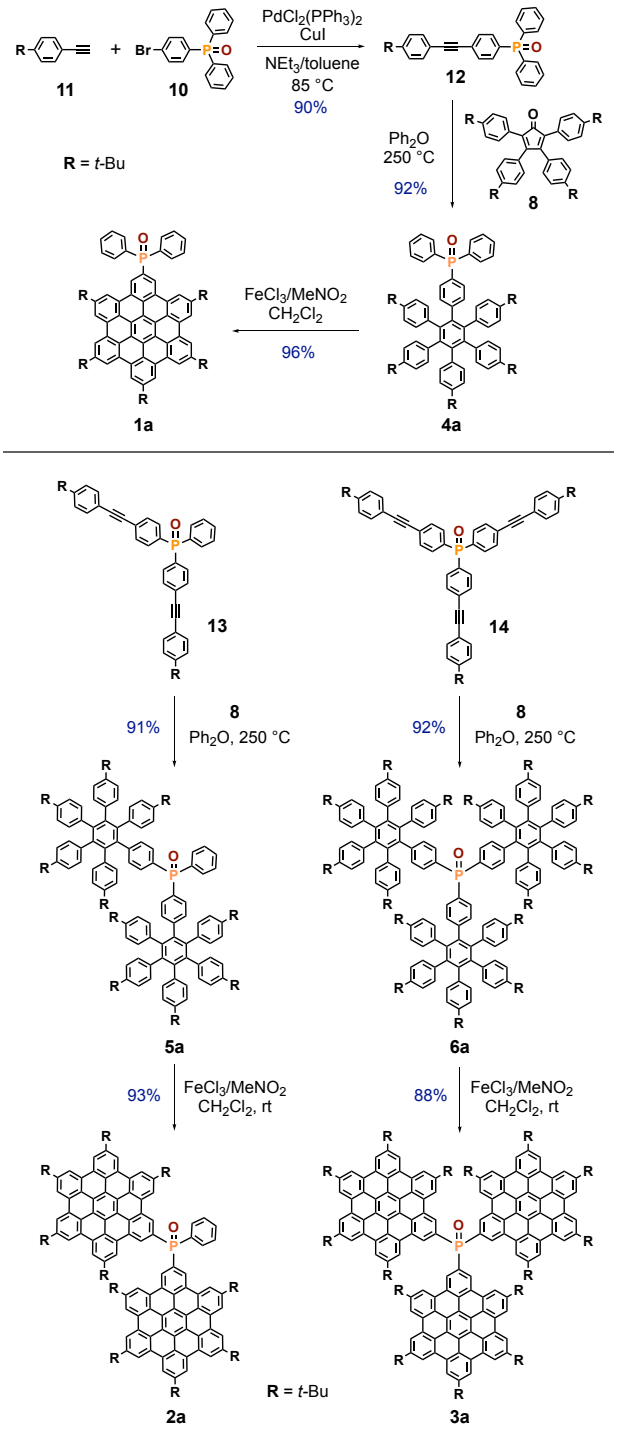

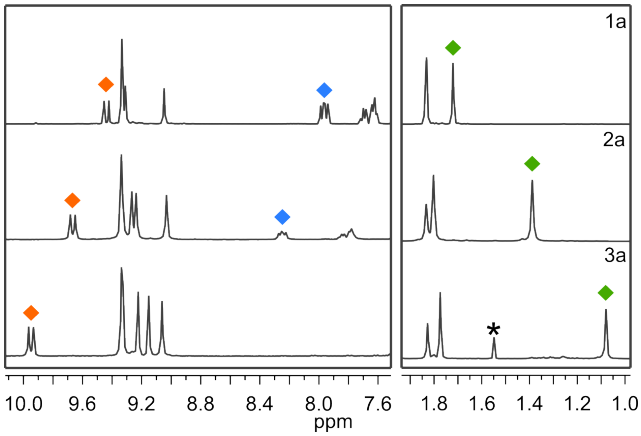

Figure 1. Cropped ^{1}H NMR spectra (500 MHz, $CDCl_3$) of phosphine oxides **1a–3a**, showing resonances arising from protons *ortho* to phosphorus labelled with orange diamonds (HBC) and blue diamonds (Ph). The *t*-Bu groups closest to phosphorus are labelled with green diamonds.

Phosphines **1–3** were prepared by the reduction of oxides **1a–3a** by $LiAlH_4$-$CeCl_3$ or diphenylsilane (Scheme 2). The $LiAlH_4$-$CeCl_3$ method[42] was complicated by the apparent reduction of the P–HBC bond, as evidenced by mass spectrometry and becoming increasingly prevalent with the more highly-substituted homologues. The milder reducing agent SiH_2Ph_2[43] showed no evidence of P–C bond cleavage (Table 1). Phosphines **1-3** were less soluble than the other phosphine adducts and could be isolated as yellow powders by precipitation from the reaction mixture with methanol. By an alternative method,[44] phosphine-borane adducts **1b–3b** were isolated and their enhanced stability and solubility allowed for easy solution phase purification. The phosphine-borane complexes were easily deprotected[45] by heating MeOH/THF mixtures, followed by removal of the volatiles *in vacuo*. The preferred approach is for the phosphines to be then reacted on *in situ*, with no evidence of phosphine oxide in the products. The superphenylphosphines have been isolated in practical quantities (>300 mg) following the efficient five-step route outlined, thereby allowing their chemistry to be further investigated on a range of fronts.

Scheme 2. Reductions to 1–3, conversion to phosphine-borane (1b–3b) and selenide (1c-3c) adducts.

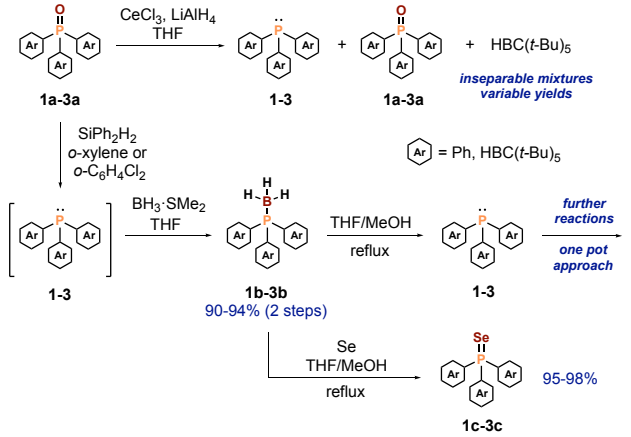

Table 1. Reduction to phosphines 1-3, borane complexes 1b-3b and their ^{31}P chemical shifts.

Reactant	Solvent	Conditions[a]	Product (yield, %)	^{31}P δ ppm
1a	*o*-xylene	a	**1** (51)	−4.2
2a	*o*-xylene	a	**2** (60)	−4.1
3a	*o*-$C_6H_4Cl_2$	a	**3** (68)	−5.3
1a	*o*-xylene	b	**1b** (94)	23.0
2a	*o*-xylene	b	**2b** (90)	24.8
3a	*o*-$C_6H_4Cl_2$	b	**3b** (92)	25.1

[a]Reaction conditions: a) **1a–3a**, SiH_2Ph_2 (33 eq.), *o*-xylene or *o*-$C_6H_4Cl_2$, 170 °C, 18 h. b) i. **1a–3a**, SiH_2Ph_2 (33 eq.), *o*-xylene or *o*-$C_6H_4Cl_2$, 170 °C, 18 h. ii. BH_3·SMe_2 (10 eq.) rt, 4 h.

Complexation with Palladium(II) Chloride. Palladium(II) chloride was chosen for complexation as it typically forms thermodynamically driven, square-planar complexes of the type $PdCl_2L_2$. It was of interest to probe the influence of the HBC fragments on isomer distribution and other structural variations across the phosphine series. Phosphine ligands **1–3** were each mixed with $PdCl_2$ in THF in a 2:1 or 1:1 ratio, returning $PdCl_2L_2$ and $Pd_2Cl_4L_2$ complexes, respectively, in near quantitative yields (Scheme 3).

Scheme 3. Synthesis of palladium(II) complexes.

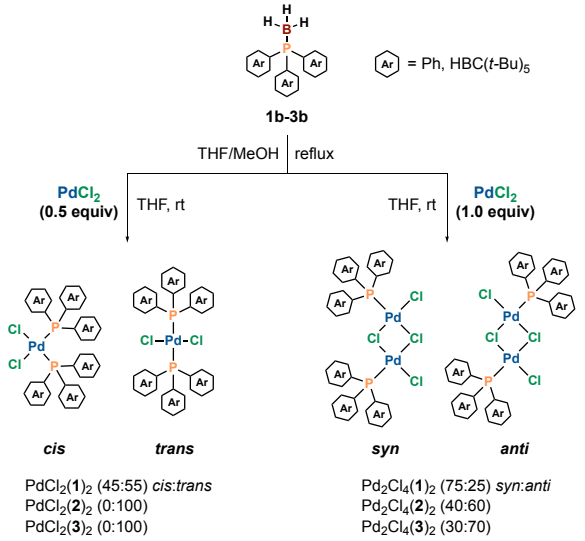

Isomers of $PdCl_2L_2$ were assigned based on distinct ^{31}P NMR resonances at ca. 35 ppm (*cis*) and ca. 20 ppm (*trans*). Crude $PdCl_2(\mathbf{1})_2$ contained a mixture of *cis* (36.6 ppm) and *trans* (21.9 ppm) isomers, while X-ray diffraction of crystals of $PdCl_2(\mathbf{1})_2$ revealed the *trans* complex (vide infra), with no evidence of the *cis* isomer after extensive crystal screening. Despite this observation, solution ^{31}P NMR of recrystallized $PdCl_2(\mathbf{1})_2$ revealed a mixture of isomers, similar in distribution to the crude material. Solid-state NMR of the recrystallized product showed the major phosphorus resonance at 15.2 ppm, consistent with the *trans* isomer being the dominant component (see Supporting Information). Thus, it appears that facile isomerization in solution affords a mixture of isomers, while the *trans* isomer is favored during crystallization,

behavior with some precedent.[46-47] ^{1}H NMR evidenced the *trans* complexes of ligands **1** and **2** with a triplet arising from protons *ortho* to phosphorus showing virtual coupling across the square-planar *bis*-phosphine complexes.[48] ^{1}H and ^{13}C NMR spectra of $PdCl_2(\mathbf{3})_2$ exhibited significant broadening of the phosphine ligand signals, particularly for atoms near the congested coordination site.

The ^{31}P spectra of the chloro-bridged dimetallic $Pd_2Cl_4L_2$ complexes each showed two resonances of similar frequency (ca. 30–33 ppm), consistent with mixtures of *syn* and *anti* isomers. With few exceptions, *bis*-monodentate phosphine $Pd_2Cl_4L_2$ complexes favor the *anti* configuration, presumably due to steric demand in the coordination sphere, while bidentate phosphines favor the *syn* isomer.[49-51] That monodentate ligands **1**–**3** all give isomeric mixtures indicates competing effects of the HBC substituents; intra-complex π–π interactions between HBC fragments act to stabilize the *syn* isomer, while the steric bulk has a destabilizing effect favoring the *anti* isomer. Assigning the ^{31}P signals as low field (*syn*) and high field (*anti*)[52] shows an increasing tendency towards the *anti* isomer across the series $Pd_2Cl_4(\mathbf{1})_2$–$Pd_2Cl_4(\mathbf{3})_2$, consistent with greater ligand steric demand. Interestingly, complex $Pd_2Cl_4(\mathbf{1})_2$—in which each ligand contains only a single HBC unit—has a strong preference for the *syn* configuration, showing that intra-complex π–π interactions are suitably favorable despite the steric bulk. For all the complexes, MALDI-TOF MS signals were assigned to fragment ions, but no molecular ions were detected due to the inherent lability of Pd(II) phosphine complexes.

Crystallographic Studies. The solid state structure, including effect of the HBC groups on molecular conformation and packing, has been investigated using X-ray crystallography for nine compounds including five complexes. The structures all contain large solvent regions that are often highly disordered (up 36% of the volume).

Crystals of the phosphine oxides **1a**–**3a** all proved amenable to X-ray diffraction. The structure of **1a** revealed an asymmetric unit containing eight independent phosphine oxide molecules arranged into four dimers around a central channel of ordered toluene and other disordered solvent molecules (Figure 2). Each dimer is orientated perpendicularly to four neighbors, interacting through a series of edge-to-face motifs. The HBC fragments of each dimer show the smallest lateral offset of all structures presented here (0.47–0.72 Å) with a rotational offset of the phosphorus moieties of ~90°. This arrangement of intermolecular HBC dimers is unusual as the first example where there is significant twisting (~30°) between the 'nanographene' planes (Figure 2a), known as turbostratic stacking in bilayer graphene.[53] The related borane **1b** (Figure 2b and Supporting Information) crystallizes in centrosymmetric face-to-face dimers with a lateral translation of 3.63 Å and the more common Bernal (AB) bilayer graphitic π-stacking.

The two HBC fragments of phosphine oxide **2a** are linked through phosphorus with an angle of 84.1° between the aromatic cores (Figure 3). Each HBC is involved in intermolecular π-interactions giving rise to extended 1-D ribbons running parallel throughout the structure. The lateral offset between interacting pairs here (3.49–3.87 Å) is typical of HBC dimers.

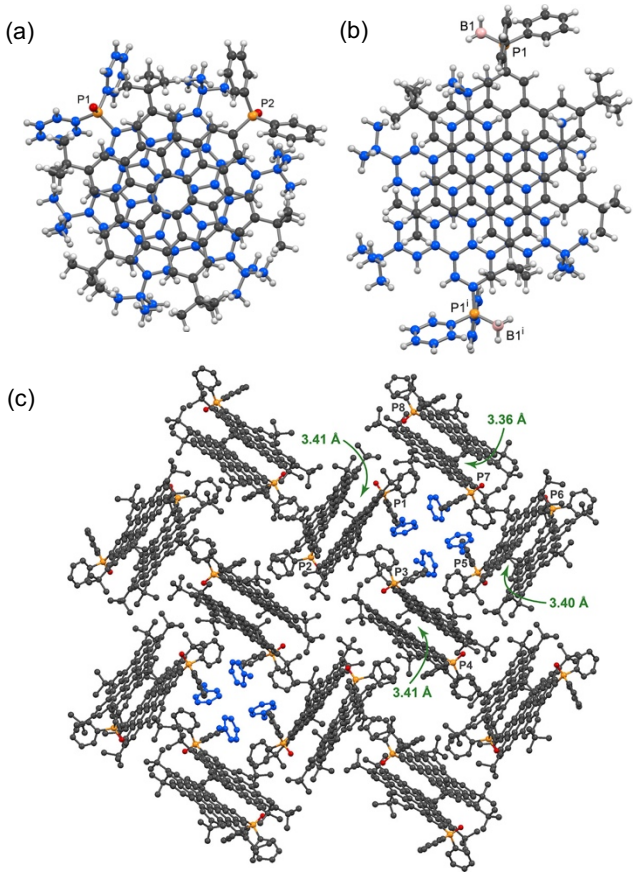

Figure 2. X-ray crystal ball and stick diagrams of (a) **1a** dimer pair, (b) **1b** dimer pair [Symmetry code: (i) 1–*x*, 1–*y*, 1–*z*], and (c) a packing diagram of **1a** viewed down the solvent channels (ordered toluene shown in blue).

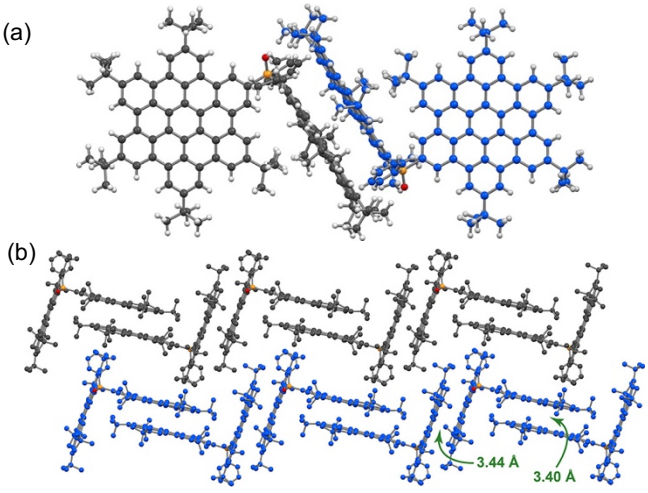

Figure 3. (a) X-ray crystal ball and stick diagram of **2a** dimer pair, and (b) two 1-D ribbons. Solvent omitted for clarity.

Molecules of **3a** adopt chiral, propeller structures with pseudo-threefold rotational symmetry about the P=O axis (Figure 4). One *t*-Bu group of each HBC sits over the face of an adjacent HBC of the same molecule. The HBC groups engage in intermolecular π-stacked dimers with

neighboring molecules of alternating orientation. Impressively, this "up-down" arrangement is repeated at each HBC in the structure, resulting in long range, 2-D layers; a sixfold supramolecular motif of the layers is shown in Figure 4b. The intermolecular interactions appear suitably strong to distort the HBC components from the idealized planar conformation, with significant curvature and twisting observed, up to 18.1° side-to-side (average 11.1°). The interplanar distance between HBC dimers for **1a**-**3a** fall in the range 3.36 Å (close to that in graphite) to 3.51 Å. Surprisingly, the C-P-C_{av} angle for the phosphine oxides **1a**-**3a** does not show a large variance (105.4–105.5°).

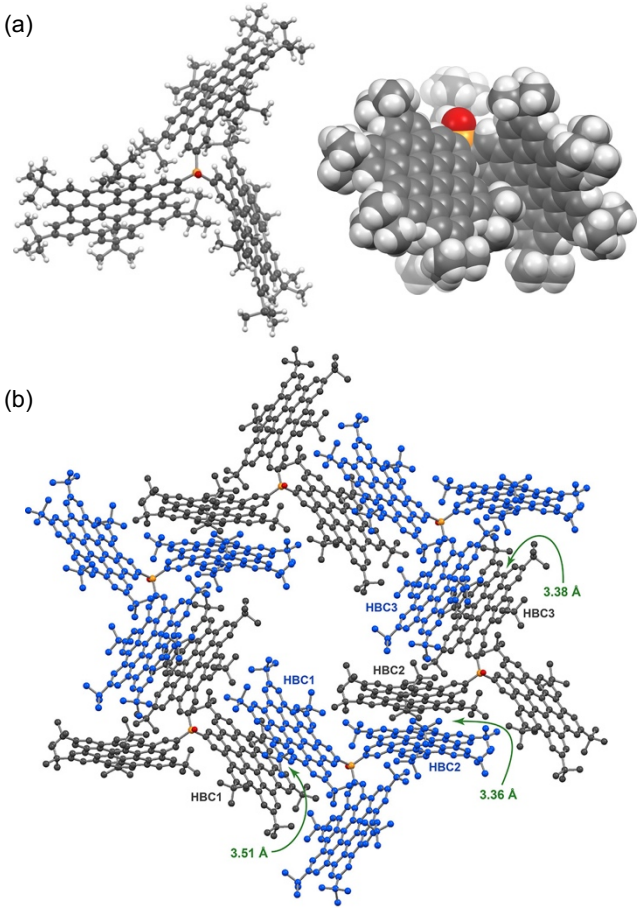

Figure 4. (a) X-ray crystal ball and stick, and space-filling diagrams of **3a**. (b) Six molecules of **3a** showing intermolecular π-stacked motif with "up (gray)-down (blue)" orientations (hydrogen atoms and solvent omitted for clarity).

Having determined that offset face-to-face π-stacking drives the assembly of the phosphine precursors, the role HBC plays in the phosphine-metal complexes was investigated next. Crystals grown from solutions of $PdCl_2$(**1**)$_2$ $PdCl_2$(**2**)$_2$, and $PdCl_2$(**3**)$_2$ were all revealed as the *trans* isomer (Figures 5). The phosphine ligands adopt a conformation such that a HBC substituent from each phosphine engages in intramolecular π-stacking with a separation of 3.40–3.43 Å. The lateral offset between the HBCs is 3.54–3.89 Å, similar to that of **2a**–**3a**; however, the constraints imposed by the metal coordination force a ~45° rotation of the P-P axis relative to the plane of the PAHs and AB-orthorhombic rather than Bernal graphitic stacking.[54]

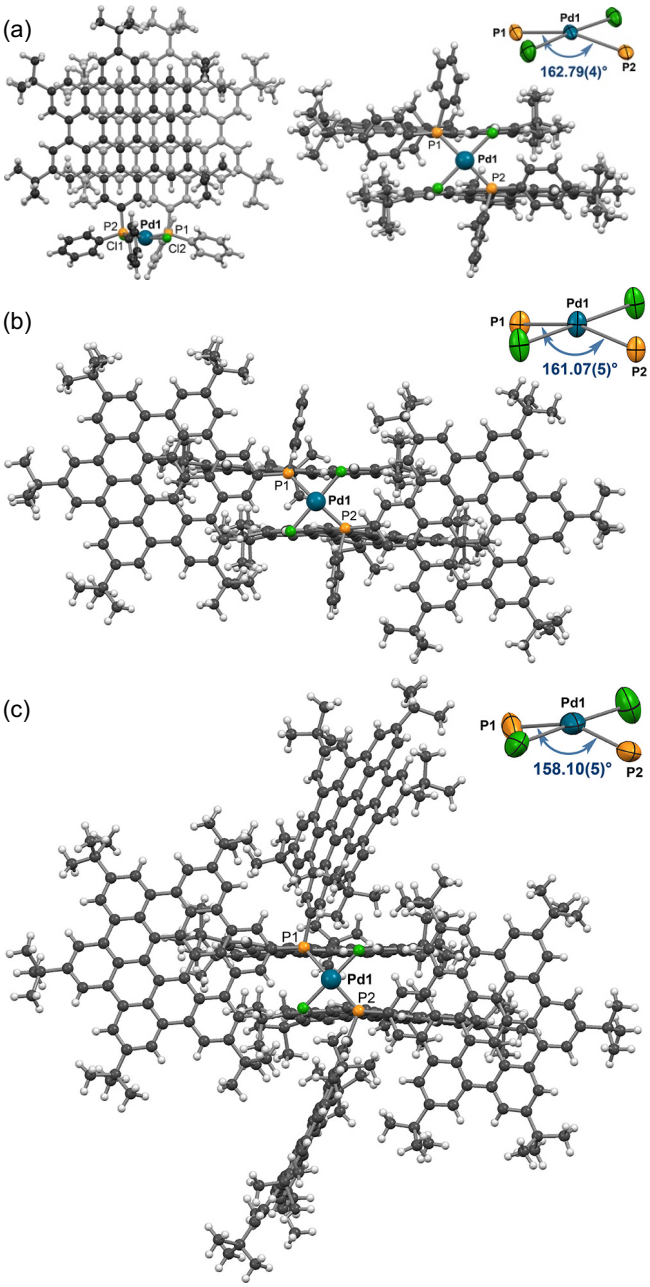

Figure 5. X-ray crystal ball and stick diagrams of (a) *trans*-$PdCl_2$(**1**)$_2$, (b) *trans*-$PdCl_2$(**2**)$_2$, (c) *trans*-$PdCl_2$(**3**)$_2$. Solvent omitted for clarity. ORTEP diagrams of the Pd coordination sphere shown as an inset with P–Pd–P angles.

The *bis*-phosphine supramolecular-chelate motif results in a distortion of the P–Pd–P angles from the idealized 180° for *trans*-$PdCl_2L_2$ complexes. The P–Pd–P angle becomes increasingly strained with growing ligand size, such that 158.10(5)° measured for $PdCl_2$(**3**)$_2$ (Figure 5c) is the most acute recorded for any *trans*-palladium(II) complex with two monodentate *P*-donor ligands.[55] This trend suggests that the coordination geometry in the solid state is influenced not only by the pseudo-chelate motif, but also solid-state intermolecular packing interactions between additional PAH substituents.

The ability of the nanographene groups to direct supramolecular order is also of interest. $PdCl_2$(**1**)$_2$—which has no 'free' HBC groups—shows a head-to-head/tail-to-

tail arrangement resulting in a lamellar arrangement of $PdCl_2(\mathbf{1})_2$ molecules interspersed by layers of chloroform solvent (Figure 6a). $PdCl_2(\mathbf{2})_2$ forms centrosymmetric dimers through π-interactions of one free HBC fragment (Figure 6b) but steric hindrance at the second HBC precludes the formation of chains as observed for related phosphine oxide **2a**. In contrast, $PdCl_2(\mathbf{3})_2$ shows interdigitated ribbons due to intermolecular π-interactions between HBCs perpendicular to the plane of the intramolecularly stacked dimer (Figure 6c). Across the series of $PdCl_2(\mathbf{1}\text{-}\mathbf{3})_2$, all the HBCs exhibit some curvature (average 8.1°), largest for a non-stacked HBC of $PdCl_2(\mathbf{3})_2$ (19.7° between peripheral rings).

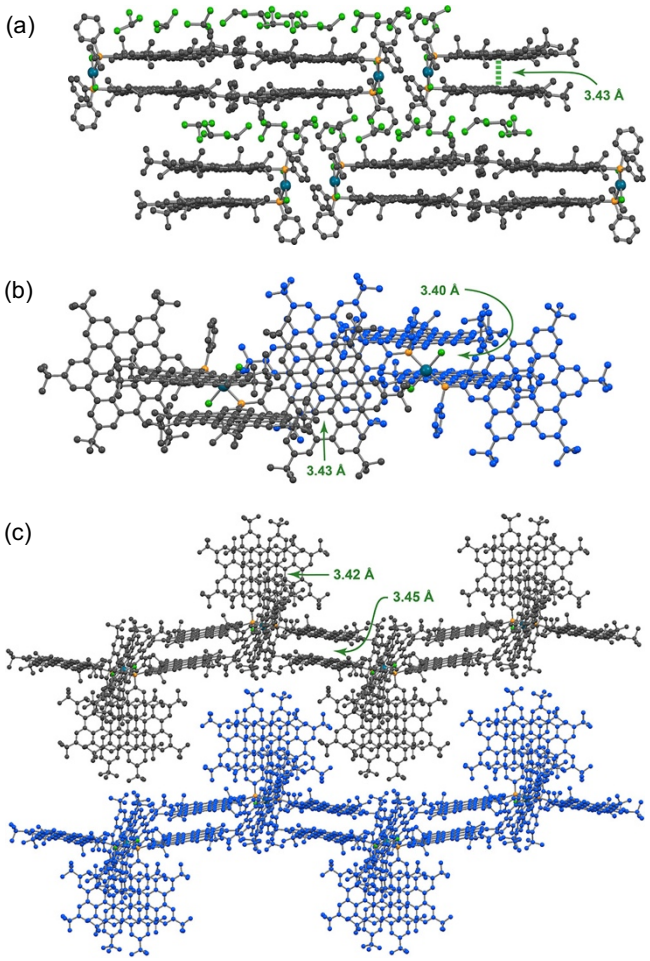

Figure 6. (a) X-ray crystal ball and stick diagram depicting long range packing arrangement for *trans*-$PdCl_2(\mathbf{1})_2$ with interlayer chloroform molecules. (b) A dimer of *trans*-$PdCl_2(\mathbf{2})_2$. (c) Two chains of *trans*-$PdCl_2(\mathbf{3})_2$. Some solvent and hydrogen atoms omitted for clarity.

The two metals of the $Pd_2Cl_4L_2$ complexes provide a less hindered coordination environment. Single crystals from $Pd_2Cl_4(\mathbf{1})_2$ and $Pd_2Cl_4(\mathbf{2})_2$ reveal the *anti* and *syn* complexes, respectively, consistent with the major isomers in solution. Despite a P···P distance of 6.186(1) Å, *anti*-$Pd_2Cl_4(\mathbf{1})_2$ (Figure 7a) adopts a close inter-HBC contact (3.40 Å) which induces significant curvature across the interacting HBCs (up to 15.9° side-to-side) and a reduction of the Pd···Pd distance to 2.9294(4) Å. This is the shortest Pd···Pd distance reported for a *bis*-monodentate phosphine $Pd_2Cl_4L_2$ complex,[55] with only a bidentate ligand complex showing greater distortion.[49]

The *syn*-configuration of $Pd_2Cl_4(\mathbf{2})_2$ permits the coordination plane to share the same axis as the interacting HBCs (Figure 17b,c). This allows for strong inter-HBC interactions without significantly distorting the coordination sphere. The intra-complex HBC stacking distance is 3.45 Å while the second HBC groups stack intermolecularly (3.37 Å), giving a supramolecular structure of 1-D ribbon motifs (Figure 7c).

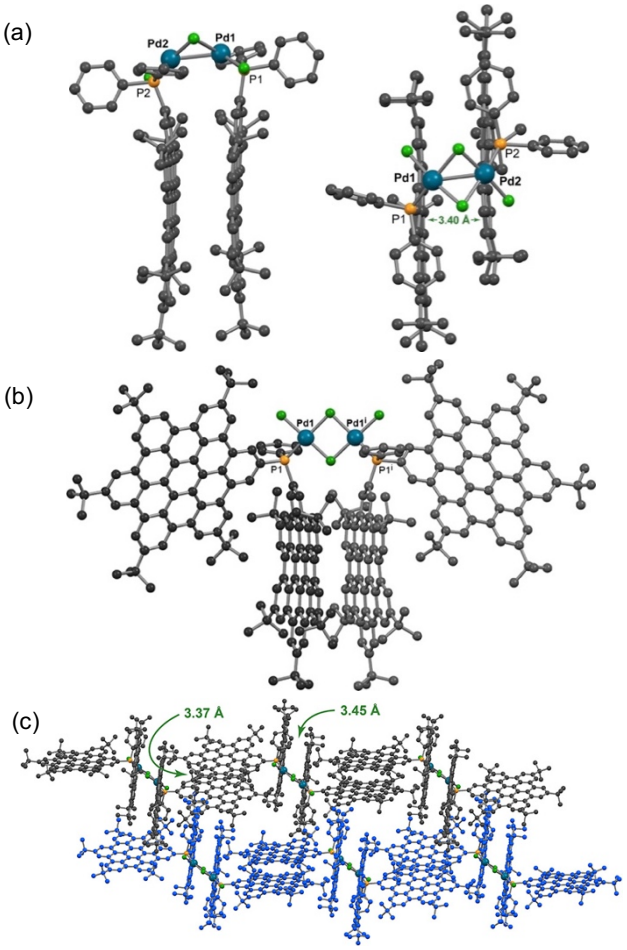

Figure 7. X-ray crystal ball and stick diagrams of (a) *anti*-$Pd_2Cl_4(\mathbf{1})_2$, (b) *syn*-$PdCl_2(\mathbf{2})_2$ [Symmetry code: (i) $-x, y, 1/2-z$], and (c) long range packing order in *syn*-$PdCl_2(\mathbf{2})_2$. Solvent and hydrogen atoms omitted for clarity.

The reliability of HBC(*t*-Bu)$_5$ as a supramolecular synthon contrasts with anthracene-based phosphines that do not always adopt an π-stacked conformation.[56] Although compelling evidence for robust, inter-HBC interactions was observed in the solid state, this structural rigidity was not replicated in solution. $PdCl_2(\mathbf{2})_2$ displayed only minor broadening for ^{1}H NMR down to –50°C , indicating that the π-π interactions remain dynamic down to this temperature (see Supporting Information). The phosphine oxides **1a**-**3a** also do not show significant concentration effects by NMR, consistent with previous studies[57] on HBC(*t*-Bu)$_6$ (see Supporting Information).

Having established that ligands **1**-**3** heavily influence coordination geometry in palladium(II) complexes, the steric demand generated within the coordination sphere was examined. Using the definition of Tolman,[58] the cone angle for phosphine **3** exceeds 250°, significantly greater than other triaryl phosphines. However, the *t*-Bu groups of HBC which define the cone angle are ca. 5 Å from the metal center, too far to generate significant strain within the coordination sphere. This is a similar situation to the 'holey' triethynylphosphines reported by Sawamura and co-workers.[59-60] To more realistically quantify ligand steric bulk, percent buried volume (%V_{bur}) was determined using SambVca.[61-62] Phosphine **3** gives a %V_{bur} of 30.7 %, not dissimilar to that of PPh_3 (29.6 %),[63] indicating that the peripheral HBC groups are too distant to impinge meaningfully at the metal. %V_{bur} for the $PdCl_2L_2$ crystal structures, where the two interacting ligands were treated as a single *trans*-chelating phosphine is 56.3–53.4%, decreasing modestly across the ligand series **1**–**3**; the second and third HBC units of ligands **2** and **3** have little influence on overall ligand steric demand. The trend towards decreasing %V_{bur} across the series was attributed to a concomitant decrease of the P–Pd–P bond angle, effectively extruding more of the ligand from the coordination sphere.

Electronic, Photophysical and Redox Properties. In preliminary experiments to assess the activity of a supertriphenylphosphine complex, $PdCl_2$(**1**)$_2$ was utilized in the Suzuki-Miyaura cross-coupling of simple aromatic substrates (see Supporting Information). The complex $PdCl_2$(**1**)$_2$ displayed catalytic activity comparable to $PdCl_2(PPh_3)_2$. To probe the electronic environment at phosphorus in **1**-**3**, $J(^{31}P–^{77}Se)$ from phosphine-selenide adducts[64-65] (Scheme 2) was measured (Table 2). $J(^{31}P–^{77}Se)$ increased with increasing number of HBC substituents suggesting that the HBC fragments have a slightly negative, additive effect on the electron donating ability of the phosphorus donor atom. However, it is unclear if this is a function of the electronics of HBC or an influence of HBC steric bulk on the geometry at phosphorus. The geometry measured crystallographically was deemed unreliable for correlation due to the major influence of inter-HBC interactions on bond angles and distances.

Table 2. ^{31}P chemical shifts and J_{PSe} coupling constants for phosphine-selenides.

Compound	^{31}P δ (ppm)	J_{PSe} (Hz)
1c	37.6	731.0
2c	38.6	734.0
3c	40.4	738.9
$SePPh_3$	35.3	729.5

^{31}P NMR spectra recorded at 162 MHz. Resonances externally referenced against PPh_3 or 85% H_3PO_4 in D_2O.

As HBC derivatives are often redox active,[25] strongly absorbing and emissive,[37] we investigated the influence of the phosphorus moiety on these properties. Analysis of cyclic voltammetric data (Table 3) across the series **1**, **1a**, **1b** and **1c** showed the first oxidation in the range 1.11–1.31 V, similar to HBC(*t*-Bu)$_6$ (1.16 V).[25] The oxidation potential of phosphine oxide **1a** was significantly higher than that of **1**, consistent with the oxide being a more electron-withdrawing substituent. Across the phosphine oxide series **1a**–**3a** a quasi-reversible process in the range 1.22–1.28 V is assigned as HBC centered since $OPPh_3$ shows no oxidation to 1.80 V. Reductions were not observed for any of the compounds studied.

Table 3. Cyclic voltammetry data for selected phosphines and their derivatives.

Compound	E^1_{pa}	E^1_{pc}	$E^1_{1/2}$	Δ
HBC(*t*-Bu)$_6$	1.16	1.07	1.12	0.08
PPh_3	1.25	-	-	-
$OPPh_3$	-	-	-	-
P[HBC(*t*-Bu)$_5$]Ph_2 (**1**)	1.11	-	-	-
H_3B·P[HBC(*t*-Bu)$_5$]Ph_2 (**1b**)	1.30	1.17	1.23	0.13
SeP[HBC(*t*-Bu)$_5$]Ph_2 (**1c**)	1.14	-	-	-
OP[HBC(*t*-Bu)$_5$]Ph_2 (**1a**)	1.31	1.12	1.22	0.18
OP[HBC(*t*-Bu)$_5$]$_2$Ph (**2a**)	1.32	1.17	1.25	0.16
OP[HBC(*t*-Bu)$_5$]$_3$ (**3a**)	1.37	1.19	1.28	0.17

Measured in 0.1 M Bu_4NPF_6 in CH_2Cl_2 at 100 mV s^{-1}. Referenced against the decamethylferrocene/decamethylferrocenium couple (–0.07 V vs SCE).

Absorption and emission spectra for the HBC-phosphines and their complexes showed spectral features consistent with mono-functionalized, HBC(*t*-Bu)$_5$R compounds[31] (see Supporting Information; representative spectra Figure 8). Mono-HBC-compounds **1**, **1a**–**1c** have absorption maxima in the range 362–364 nm, and profiles that show the phosphorus has little influence on the HBC chromophore. Emission maxima were similar across the series with all compounds exhibiting strong green emission. Phosphine oxides showed only subtle red-shifting across the series (362 (**1a**)–364 (**3a**) nm), however, molar absorptivity displayed a dramatic, additive effect with increasing number of HBC chromophores (Figure 8b), also observed for the Pd complexes (Figure 8c).

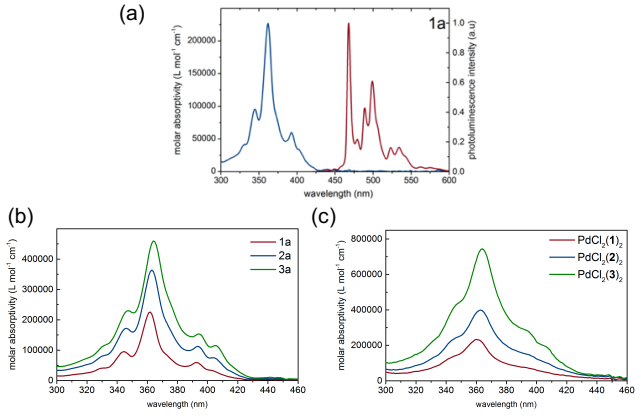

Figure 8. (a) Absorption and emission spectra of **1a**. (b) Absorption spectra of the series **1a**–**3a**. (c) Absorption spectra of the complexes $PdCl_2$(**1**)$_2$–$PdCl_2$(**3**)$_2$.

CONCLUSION

A series of triarylphosphines bearing 1–3 HBC units have been synthesized in excellent yields (50-74% over ≤5 steps). The divergent route allows the preparation of the soluble phosphine oxide precursors on a gram scale. Mirroring the behaviour of simple HBC compounds, the ligands are strong chromophores (absorption and green emission) and redox active. To demonstrate the utility of the superphenylphosphines as ligands, the complexes $PdCl_2L_2$ and $Pd_2Cl_4L_2$ were prepared and characterised in solution and the solid state. The HBC substituents impart constraints on the coordination geometry and conformation of complexes bearing the phosphine ligands. In all five crystal structures of the complexes, robust intramolecular HBC···HBC π–stacking dominates the ligand sphere, functioning as supramolecular bidentate-like ligands. The strength of the intramolecular interaction manifests through an unusually short Pd···Pd separation in the complex $Pd_2Cl_4(\mathbf{1})_2$ and record distortion of the P–Pd–P angle in *trans*-$PdCl_2(\mathbf{3})_2$. The multi-HBC ligands **2** and **3** drive long range supramolecular order to porous solids, facilitated by the additional HBC substituents. The functionalization chemistry of HBCs is now relatively mature and presents an exciting opportunity to further explore the coordination, organometallic and supramolecular chemistry of superphenylphosphines.

ASSOCIATED CONTENT

Supporting Information. Synthesis procedures and characterization data; NMR, MALDI-TOF MS, UV-visible/fluorescence spectra; cyclic voltammetry traces; catalysis experiments; X-ray crystallography details and ORTEP diagrams; $\%V_{bur}$ calculations and steric maps (PDF). Crystallographic data for all reported structures (CIF).

AUTHOR INFORMATION

Corresponding Author

*E-mail: nlucas@chemistry.otago.ac.nz.

Author Contributions

The manuscript was written through contributions of all authors. All authors have given approval to the final version of the manuscript.

Notes

The authors declare no competing financial interest.

ACKNOWLEDGMENT

Financial support was provided by the University of Otago (Department of Chemistry, University of Otago Research Grants scheme) and the MacDiarmid Institute for Advanced Materials and Nanotechnology. J.N.S. thanks the University of Otago for a Doctoral Scholarship.

ABBREVIATIONS

HBC, hexa-*peri*-hexabenzocoronene, hexabenzo[*bc*,*ef*,*hi*,*kl*,-*no*,*qr*]coronene; HPB, hexaphenylbenzene.

REFERENCES

1. Quin, L. D., *A Guide to Organophosphorus Chemistry*. Wiley: New York, 2000.
2. Peters, J.; Thomas, J. C., Ligands, Reagents, and Methods in Organometallic Synthesis. In *Comprehensive Organometallic Chemistry III*, Crabtree, R. H.; Mingos, D. M. P., Eds. Elsevier Science: New York, 2007; Vol. 1.
3. Burt, J.; Levason, W.; Reid, G., *Coord. Chem. Rev.* **2014,** *260*, 65.
4. Kamer, P. C. J.; van Leeuwen, P. W. N. M., *Phosphorus(III) Ligands in Homogeneous Catalysis: Design and Synthesis*. John Wiley & Sons: Chichester, UK, 2012.
5. James, S. L., *Chem. Soc. Rev.* **2009,** *38*, 1744.
6. Johnson, G. E.; Laskin, J., *Analyst* **2016,** *141*, 3573.
7. Stephan, D. W., *Acc. Chem. Res.* **2015,** *48*, 306.
8. Jeon, S. O.; Lee, J. Y., *J. Mater. Chem.* **2012,** *22*, 4233.
9. Shameem, M. A.; Orthaber, A., *Chem. – Eur. J.* **2016,** *22*, 10718.
10. Birkholz, M. N.; Freixa, Z.; van Leeuwen, P. W. N. M., *Chem. Soc. Rev.* **2009,** *38*, 1099.
11. Breit, B.; Seiche, W., *J. Am. Chem. Soc.* **2003,** *125*, 6608.
12. Köpfer, A.; Breit, B., *Angew. Chem. Int. Ed.* **2015,** *54*, 6913.
13. Raynal, M.; Ballester, P.; Vidal-Ferran, A.; van Leeuwen, P. W. N. M., *Chem. Soc. Rev.* **2014,** *43*, 1660.
14. Slagt, V. F.; Röder, M.; Kamer, P. C. J.; van Leeuwen, P. W. N. M.; Reek, J. N. H., *J. Am. Chem. Soc.* **2004,** *126*, 4056.
15. Neel, A. J.; Hilton, M. J.; Sigman, M. S.; Toste, F. D., *Nature* **2017,** *543*, 637.
16. Dance, I., π-π Interactions: Theory and Scope. In *Encyclopedia of Supramolecular Chemistry*, Atwood, J. L.; Steed, J. W., Eds. CRC Press: New York, USA, 2004; Vol. 2, pp 1076.
17. Dance, I.; Scudder, M., *CrystEngComm* **2009,** *11*, 2233.
18. Desiraju, G. R.; Gavezzotti, A., *J. Chem. Soc., Chem. Commun.* **1989,** 621.
19. Goddard, R.; Haenel, M. W.; Herndon, W. C.; Krüger, C.; Zander, M., *J. Am. Chem. Soc.* **1995,** *117*, 30.
20. Sergeyev, S.; Pisula, W.; Geerts, Y. H., *Chem. Soc. Rev.* **2007,** *36*, 1902.
21. Wöhrle, T.; Wurzbach, I.; Kirres, J.; Kostidou, A.; Kapernaum, N.; Litterscheidt, J.; Haenle, J. C.; Staffeld, P.; Baro, A.; Giesselmann, F.; Laschat, S., *Chem. Rev.* **2016,** *116*, 1139.
22. Tracz, A.; Jeszka, J. K.; Watson, M. D.; Pisula, W.; Müllen, K.; Pakula, T., *J. Am. Chem. Soc.* **2003,** *125*, 1682.
23. Wu, J.; Pisula, W.; Müllen, K., *Chem. Rev.* **2007,** *107*, 718.
24. Clar, E.; Ironside, C. T., *Proc. Chem. Soc., London* **1958,** 150.
25. Herwig, P. T.; Enkelmann, V.; Schmelz, O.; Müllen, K., *Chem. – Eur. J.* **2000,** *6*, 1834.
26. Watson, M. D.; Fechtenkötter, A.; Müllen, K., *Chem. Rev.* **2001,** *101*, 1267.
27. Clar, E., *The Aromatic Sextet*. John Wiley & Sons: London, 1972.
28. Ito, S.; Herwig, P. T.; Böhme, T.; Rabe, J. P.; Rettig, W.; Müllen, K., *J. Am. Chem. Soc.* **2000,** *122*, 7698.
29. Feng, X.; Pisula, W.; Zhi, L.; Takase, M.; Müllen, K., *Angew. Chem. Int. Ed.* **2008,** *47*, 1703.
30. Lungerich, D.; Hitzenberger, J. F.; Marcia, M.; Hampel, F.; Drewello, T.; Jux, N., *Angew. Chem. Int. Ed.* **2014,** *53*, 12231.
31. El Hamaoui, B.; Laquai, F.; Baluschev, S.; Wu, J.; Müllen, K., *Synth. Met.* **2006,** *156*, 1182.
32. Kim, K.-Y.; Liu, S.; Köse, M. E.; Schanze, K. S., *Inorg. Chem.* **2006,** *45*, 2509.
33. El Hamaoui, B.; Zhi, L.; Wu, J.; Li, J.; Lucas, N. T.; Tomović, Ž.; Kolb, U.; Müllen, K., *Adv. Funct. Mater.* **2007,** *17*, 1179.

34. Woolf, A.; Chaplin, A. B.; McGrady, J. E.; Alibadi, M. A. M.; Rees, N.; Draper, S.; Murphy, F.; Weller, A. S., *Eur. J. Inorg. Chem.* **2011,** 1614.
35. Roberts, D. J.; Nolan, D.; Máille, G. M. Ó.; Watson, G. W.; Singh, A.; Ledoux-Rak, I.; Draper, S. M., *Dalton Trans.* **2012,** *41*, 8850.
36. Nolan, D.; Gil, B.; Wang, L.; Zhao, J.; Draper, S. M., *Chem. – Eur. J.* **2013,** *19*, 15615.
37. Elliott, A. B. S.; Horvath, R.; Sun, X.-Z.; Gardiner, M. G.; Müllen, K.; Lucas, N. T.; George, M. W.; Gordon, K. C., *Inorg. Chem.* **2016,** *55*, 4710.
38. Wright, J. R.; Crowley, J. D.; Lucas, N. T., *Chem. Commun.* **2016,** *52*, 12976.
39. Draper, S. M.; Gregg, D. J.; Schofield, E. R.; Browne, W. R.; Duati, M.; Vos, J. G.; Passaniti, P., *J. Am. Chem. Soc.* **2004,** *126*, 8694.
40. Gregg, D. J.; Fitchett, C. M.; Draper, S. M., *Chem. Commun.* **2006,** 3090.
41. Stępień, M.; Gońka, E.; Żyła, M.; Sprutta, N., *Chem. Rev.* **2017,** *117*, 3479.
42. Imamoto, T.; Takeyama, T.; Kusumoto, T., *Chem. Lett.* **1985,** *14*, 1491.
43. Hérault, D.; Nguyen, D. H.; Nuel, D.; Buono, G., *Chem. Soc. Rev.* **2015,** *44*, 2508.
44. Schirmer, M.-L.; Jopp, S.; Holz, J.; Spannenberg, A.; Werner, T., *Adv. Synth. Catal.* **2016,** *358*, 26.
45. Van Overschelde, M.; Vervecken, E.; Modha, S. G.; Cogen, S.; Van der Eycken, E.; Van der Eycken, J., *Tetrahedron* **2009,** *65*, 6410.
46. Bodenhausen, G.; Deli, J. A.; Anklin, C.; Pregosin, P. S., *Inorg. Chim. Acta* **1983,** *77*, L17.
47. Real, J.; Prat, E.; Polo, A.; Álvarez-Larena, Á.; Piniella, J. F., *Inorg. Chem. Commun.* **2000,** *3*, 221.
48. Pidcock, A., *Chem. Commun.* **1968,** 92.
49. Konrad, T. M.; Fuentes, J. A.; Slawin, A. M. Z.; Clarke, M. L., *Angew. Chem. Int. Ed.* **2010,** *49*, 9197.
50. Awada, M.; Jeunesse, C.; Matt, D.; Toupet, L.; Welter, R., *Dalton Trans.* **2011,** *40*, 10063.
51. Takeda, N.; Tagawa, T.; Unno, M., *Heteroat. Chem.* **2014,** *25*, 628.
52. Smith, J. D. C.; Lake, C. H.; Gray, G. M., *Dalton Trans.* **2003,** 2950.
53. Fang, W.; Hsu, A. L.; Song, Y.; Kong, J., *Nanoscale* **2015,** *7*, 20335.
54. Savini, G.; Dappe, Y. J.; Öberg, S.; Charlier, J.-C.; Katsnelson, M. I.; Fasolino, A., *Carbon* **2011,** *49*, 62.
55. Groom, C. R.; Bruno, I. J.; Lightfoot, M. P.; Ward, S. C., *Acta Crystallogr., Sect. B* **2016,** *72*, 171.
56. Yang, F.; Fanwick, P. E.; Kubiak, C. P., *Inorg. Chem.* **2002,** *41*, 4805.
57. Kastler, M.; Pisula, W.; Wasserfallen, D.; Pakula, T.; Müllen, K., *J. Am. Chem. Soc.* **2005,** *127*, 4286.
58. Tolman, C. A., *Chem. Rev.* **1977,** *77*, 313.
59. Ochida, A.; Ito, H.; Sawamura, M., *J. Am. Chem. Soc.* **2006,** *128*, 16486.
60. Ochida, A.; Sawamura, M., *Chem. – Asian J.* **2007,** *2*, 609.
61. Poater, A.; Cosenza, B.; Correa, A.; Giudice, S.; Ragone, F.; Scarano, V.; Cavallo, L., *Eur. J. Inorg. Chem.* **2009,** *2009*, 1759.
62. Poater, A.; Ragone, F.; Giudice, S.; Costabile, C.; Dorta, R.; Nolan, S. P.; Cavallo, L., *Organometallics* **2008,** *27*, 2679.
63. Clavier, H.; Nolan, S. P., *Chem. Commun.* **2010,** *46*, 841.
64. Adams, D. J.; Bennett, J. A.; Duncan, D.; Hope, E. G.; Hopewell, J.; Stuart, A. M.; West, A. J., *Polyhedron* **2007,** *26*, 1505.
65. Allen, D. W.; Taylor, B. F., *J. Chem. Soc., Dalton Trans.* **1982,** 51.

Authors are required to submit a graphic entry for the Table of Contents (TOC) that, in conjunction with the manuscript title, should give the reader a representative idea of one of the following: A key structure, reaction, equation, concept, or theorem, etc., that is discussed in the manuscript. Consult the journal's Instructions for Authors for TOC graphic specifications.

Insert Table of Contents artwork here